Talanta 282 (2025) 126957

Contents lists available at ScienceDirect

Talanta

journal homepage: www.elsevier.com/locate/talanta

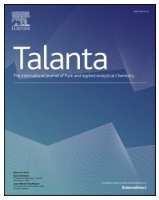

A paper-based organic electrochemical transistor array with a simplified configuration for simultaneous multi-ion detection

Ariadna Dasca, Pascal Blondeau, Jordi Riu **, Francisco J. Andrade *

Departament de Química Analítica i Química Orgànica Universitat Rovira i Virgili (URV), c/Marcel·lí Domingo 1, 43007, Tarragona, Spain

ARTICLE INFO

Handling Editor: Agata Michalska

Keywords:
Transistor array
Organic electrochemical transistor
Paper-based sensors
Chemometrics
Saliva

ABSTRACT

In recent years, organic electrochemical transistors (OECTs) have emerged as a promising tool to add to current analytical methods due to their high-amplification capacities, robust analytical performance, and versatility. The present work proposes a compact multi-analyte transistor array with outstanding analytical performance. The ion-selective organic electrochemical transistors (IS-OECTs) were developed by combining the thick-film technology with the optimum ion-selective membrane, resulting in highly sensitive and selective IS-OECTs. The system has then been simplified using only a power supply for each OECT and a single gate electrode. To prove these advantages, the IS-OECT array of sensors has been combined with multivariate models to simultaneously detect and quantify sodium, potassium and ammonium ions in human saliva. The results obtained have been validated against reference techniques, showing promising results and confirming the usefulness of the newly developed sensing array.

1. Introduction

The determination of ions in solution plays a very important role in many different fields, such as food production, healthcare, environmental monitoring, industrial applications, and water treatment, among others. Current laboratory tools to address these needs provide suitable sensitivity and linear ranges, resilience to complex matrices, and high sample throughput [1,2]. Atomic spectrometry techniques have become one of the gold standards for the determination of a wide range of ions due to their outstanding analytical performance, robustness, and the multi-elemental detection capabilities. As a major downside, however, the instrumentation required is bulky, expensive, and needs a significant degree of expertise to operate. Additionally, these techniques may show a limited linear range. For these reasons, they are normally used for a large volume of samples. Furthermore, the determination of some key cations, such as ammonium, is not possible and complementary tools -such as colorimetric determinations- must be employed [3]. Ion chromatography, on the other hand, provides an alternative way to detect a virtually unlimited range of ions over a wide concentration range. However, the analytical procedure is more tedious, and the method is slower. In this context, electrochemical sensors have gained popularity since they provide complementary advantages. Potentiometric measurements using ion-selective electrodes (ISEs) provide a way to determine a broad range of ions over a wide concentration range [4]. Due to their robust performance, ISEs have become one of the workhorses of the clinical labs. Nowadays, the determination of ions such as Na^+, K^+, Cl^-, etc., in biological fluids is routinary performed using ISEs [5]. Unlike other approaches, the instrumentation required is very compact, affordable, simple to operate and can be more easily adapted to deal with a low number of samples.

Because of all these attributes, electrochemical sensors have received a renewed interest during the last decade. This has been largely due to the growing demand for platforms to generate chemical information in the point of need [6]. The digital transformation of healthcare, for example, requires sensors to remotely check the health status of people. These technologies have the power to radically turn the current (reactive) healthcare systems into a new personalized, predictive, and preventive approach. To be implemented, however, these systems require (bio)chemical sensors that simultaneously provide a suitable analytical performance, simplicity of operation, and affordable cost. Unlike lab-based tools, the point of care needs analytical devices that can be produced and operated at mass level. Electrochemical systems are ideally suited to fulfil these needs.

For that reason, wearable and disposable devices using different

* Corresponding author.
** Corresponding author.
E-mail addresses: jordi.riu@urv.cat (J. Riu), franciscojavier.andrade@urv.cat (F.J. Andrade).

https://doi.org/10.1016/j.talanta.2024.126957
Received 30 May 2024; Received in revised form 20 September 2024; Accepted 24 September 2024
Available online 1 October 2024

kinds of electrochemical detection have been reported during the last decade [7]. The use of ISEs for the detection of ions in the point of need has been extensively explored. ISEs have been fabricated using commodity materials, such paper, plastics, rubber, etc. These systems have been incorporated into adhesive patches, yarns, band-aids, temporary tattoos, etc. The application of these devices for healthcare, water monitoring, sports performance, dehydration and general wellbeing has been demonstrated [8–11]. There are two problems that must be faced when using ISEs. First, some issues of selectivity when dealing with specific interferences. For example, due to their similar charge-radius ratio, K^+ and NH_4^+ produce a mutual interference effect. These types of problems can be minimized using multichannel systems allowing the simultaneous determination of multiple ions together with correction algorithms. A second issue is that ISEs sensitivity is limited by the Nernstian dependence. As a result, changes that are clinically highly relevant are translated into very small differences in the analytical signal. Thus, their use requires highly controlled conditions that are difficult to recreate in the point of need. Alternative solutions with higher sensitivity in the range of interest will be an invaluable tool in distributed sensing.

The organic electrochemical transistor (OECT) is a relatively recent type of chemical sensor that shows promise as a tool for the point of need. Like any transistor, OECTs have a 3-electrodes setup: source (S), drain (D), and gate (G) (Fig. 1A–B) [12]. S and D are connected through a channel made of an organic semiconductor, typically poly(3, 4-ethylenedioxythiophene)-poly(styrene sulfonate) (PEDOT:PSS). The G and the semiconducting channel are electrically connected through an electrolyte solution where they are both immersed. The system works under 2 gradients of electrical potential. The first is created by grounding the S and applying a constant negative voltage to D (V_d). This generates an electrical current (I_d) due to the high concentration of high mobility holes in the PEDOT:PSS. A second gradient of electrical potential is created by positively biasing G against the channel (V_g). This gradient induces the migration of cations from the solution into the channel [13]. The incorporation of positive ions into the channel reduces the number of holes, decreasing the electrical conductivity [14]. As a result, changes in V_g produce changes in I_d, i.e., the channel current follows the V_g. Thus, OECTs allow ion-to-electron transduction with a high-power amplification using a relatively simple setup [15]. By suitable functionalization of the gate or the channel, OECTs have been used mostly for the detection of organic compounds and all sort of biomolecules. Furthermore, the development of disposable and wearable OECT biosensors has shown the potential of this technology as a tool for the point of need. Our group, for example, has recently introduced the thick-channel approach to create OECT sensors with an exquisite sensitivity that can be built on a paper substrate using simple printing techniques [16,17].

During the last few years significant efforts have been devoted to extending the use OECTs for the detection of ions. The pioneer works of Bobacka *et al.* [18] and Malliaras *et al.* [12,19] using ion-selective membranes (ISMs) to create OECTs have resulted in the first ion-selective organic electrochemical transistors (IS-OECTs). While the concept was promising, the performance of these devices was modest. Following these lines, we have recently proposed an approach to enhance the sensitivity of the IS-OECT by suitable optimization of the ISM in combination with the thick-film channel technology [17]. This approach was used for the development of a paper based IS-OECT for the detection of K^+ in artificial serum. This simple device, which displays a sensitivity up to 5 times higher than conventional ISEs, holds promise to build devices for the point of need.

There are two interesting features of these thick-film IS-OECTs with significant practical implications. First, the use of a functionalized channel. Conventional OECTs work with a functionalized gate, which means that the simultaneous detection of multiple substances requires using multiple transistors working independently on different solutions. Functionalization of the channel, on the other hand, enables the multiplex advantage, since a generic Ag/AgCl gate could be used several channels working simultaneously in the same problem solution. The second unique feature is that under optimized conditions V_g is very close to 0 V. This means that the gate electrode could be virtually grounded and incorporated into the S. This would allow the elimination of an additional power supply, reducing the size and complexity of the instrumentation. Combining these features in a new device would provide significant advantages.

This work is devoted to the development of a multiplex IS-OECT with a simplified instrumentation and a compact setup (Fig. S1). A single Ag/AgCl electrode is used as a generic gate to simultaneously control three different channels functionalized with suitable ISM. As a proof of concept, this system is applied to the simultaneous detection of K^+, Na^+ and NH_4^+ in saliva. The determination of these cations is highly relevant for the diagnostics, control, and prevention of diseases such as periodontal disease [20], kidney disease [21], cystic fibrosis [22] or cardiovascular disease [23], among others [24,25]. The individual optimization of each one of these sensors is first performed, and then the integration of these sensors into a single array with multiple detection capabilities is carried out. Previous studies have shown the advantages of chemometrics together with multi-ion-selective electrodes (electronic tongue) [4,26], since it helps to enhance the selectivity of the system. Thus, this work also incorporates the use of multivariate models [5] to improve the results and demonstrate the advantages of multiplexing. To illustrate this concept, determination of ions in saliva has been performed. Saliva contains a large number of ions, proteins and peptides that makes it a potential source of biomarkers. The use of saliva as a sample for the prevention and control of diseases has been investigated

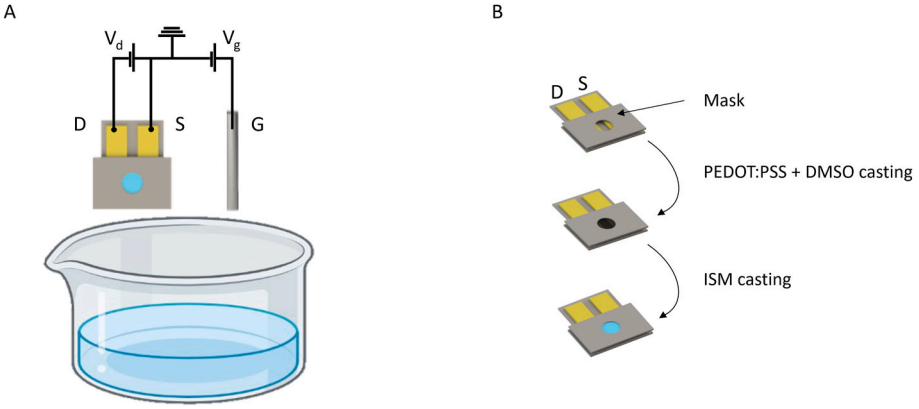

Fig. 1. (A) Illustration of the typical components of an OECT and its electrical circuit. (B) Schematics of the construction of the channel (D: drain, S: source, PEDOT:PSS: poly(3,4-ethylenedioxythiophene)-poly(styrene sulfonate), DMSO: dimethyl sulfoxide, ISM: ion-selective membrane).

in different areas since sampling is simple, non-invasive and low-cost [23]. In this way, with the use of portable point-of-care sensors that can be autonomously used by the patient, telemedicine would allow the doctor-patient relationship to take place remotely, thus reducing transport, hospital unnecessary loading and favoring personalized medical care [27]. These preliminary results show the possibility of simultaneously detecting ions with an acceptable level of accuracy. We demonstrate the precision of an array of OECTs for the determination of K^+, Na^+ and NH_4^+ in real samples of saliva, showing that the results provided by the array of OECTs are comparable to the results of three different reference methods for the determination of these ions. These achievements hold significant promise for the future of biosensor technology, opening new and attractive avenues for the development of point-of-care sensors in health and wellness applications.

2. Experimental section

2.1. OECT preparation

2.1.1. Channel fabrication

Details of the fabrication of the thick-film OECT can be found elsewhere [17]. Briefly, to make the S and D electrodes a 0.5 mm wide adhesive tape is initially placed on a photographic paper (Fig. 1B). Then, a 100 nm layer of gold is sputtered. When the adhesive tape is removed, a non-conductive gap between two gold pads is created. These two pads will act as the S and D electrodes. Thereafter, a water-resistant adhesive mask is placed on top, leaving exposed only a 3 mm diameter window. To create the channel, 1.5 μL of a filtered PEDOT:PSS solution is drop cast onto the window, covering all the exposed area. This is then dried in an oven (100 °C, 20 min). To enhance the channel conductivity, 1 μL of dimethyl sulfoxide (DMSO) is added to the window, then dried again (100 °C, 15 min) [28] and then rinsed with distilled water.

Before functionalization, the channel is conditioned in a 10^{-2} M XCl (where X corresponds to the cation, either K^+, Na^+ or NH_4^+) under constant stirring for 2 h. Finally, the channel is rinsed and left to dry for 3 h at room temperature.

0.2 and 0.4 % PEDOT:PSS dilutions were prepared by suitable dilution with distilled water of a commercial 0.8 % PEDOT:PSS solution.

2.1.2. Preparation of the ion-selective membrane cocktail

The optimal composition of the ion-selective membrane (ISM) was selected based on result of a previous work [17]. In essence, a membrane with a reduced amount of polymer matrix (compared to conventional ISM), produces a better response since the electrical permittivity of the membrane is reduced and ion transport is improved. A schematic of phase boundary potential can be found in Fig. S2. Potassium tetrakis (4-chlorophenyl) borate (0.5 mg) was used as ion exchanger. Potassium ionophore I, ammonium ionophore I, sodium ionophore X, in all cases 2 mg were used as ionophores. The polymeric matrix consists of poly(vinyl chloride) (10.9 mg) and 2-nitrophenyl octyl ether (21.6 mg) as plasticizer. Tetrahydrofuran (1 mL/35 mg) was used to dissolve all the components. These ISMs cocktails are stored in the fridge at 8 °C.

2.1.3. Sensor fabrication

Functionalization is carried out by casting ISM cocktail onto the channel. A 5 μL aliquot of the ISM cocktail is drop cast and let dry for 5 min. This process is repeated until a total of 15 μL of the cocktail have been added. The functionalized channel is let dry overnight (Fig. 1A) and before measurements, it is conditioned by immersion in a 10^{-1} M XCl (X corresponds to each cation, either K^+, Na^+ or NH_4^+) for 1 h and is then rinsed with distilled water. Fig. 2A shows the schematics of the sensor array.

For all experiments, a 2 mm diameter Ag/AgCl flat tip probe (Warner instruments, 641311) was used as the gate electrode.

The static resistance of the channel was evaluated during the preparation as a way to control the process (Fig. S3), since the resistance the channels correlates well with the final analytical performance of the system.

2.2. Electrochemical measurements

All the experiments have been performed using a 0.1 M $MgCl_2$ solution as a background electrolyte to avoid any effect due to changes on the ionic strength. The sensing array is built using three different functionalized channels (one for each analyte) and a single gate, as shown in Fig. 2B. For the electrical connections, the source electrode of each transistor, together with the gate, are connected to a common ground. Then the drain electrode (D) of each transistor is connected to an independent power supply (P, Fig. 2B). An individual ammeter is placed in series with each transistor to measure the current that flows between S and D. The gate is also connected to the common ground, since it has been previously shown that maximum transconductance is found for $V_{gMAX} = 0$ V.

The mechanism governing the polarization of the membrane-

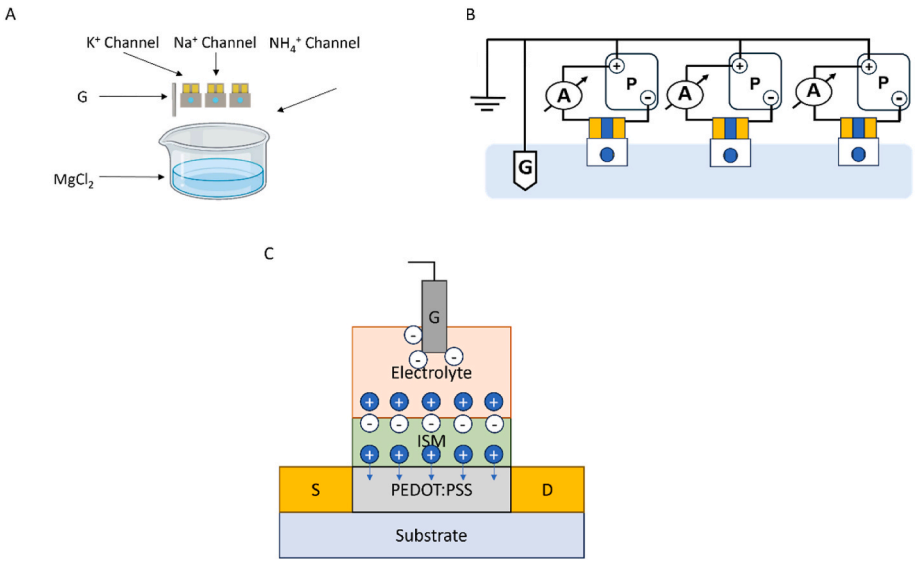

Fig. 2. (A) Schematic of the array: three functionalized channels sharing one Ag/AgCl gate. (B) Diagram of the electrical connections of system. (C) Description of an OECT. In all cases S = Source, D = Drain, and G = Gate. P = power supply.

electrolyte interface plays a critical role in the sensor's response [29]. It's important to note that both, the internal (PEDOT:PSS/membrane) and the external (membrane/solution) interfaces generate their own charge density and corresponding potential profiles (Fig. 2C and Fig. S2).

2.3. Data processing

PLS Toolbox 9.0 (Eigenvector Inc, Manson, WA, USA) running on MATLAB R2022b (Mathworks Inc., Natick, MA, USA) was used for data analysis. Partial Least Squares (PLS) regression was used for quantitative analysis. Data from the three recorded I_d values (ammonium, potassium and sodium) were used to build the **X** matrix. The concentration of each analyte was used to create each independent **Y** matrix, so an independent PLS model was calculated for each analyte. The concentration was expressed as the logarithm of concentration. Data were autoscaled before the construction of the PLS model. Venetian blinds (with 9 data splits and 2 samples per blind) was used for the cross-validation of the training set. The training set was independent of the test set, which consists of 22 samples.

2.4. Analysis of the synthetic and real samples by the OECTs array

The training set, the test set and the real samples were analyzed with the designed transistor array. For the training set and test set samples, different standard solutions of cations in the electrolyte media were added. Then, the current value after each addition was measured. To take into account real measurement conditions, the analysis was performed on a total of 20 OECTs for each analyte and on different days. For real samples, a total of 7 OECTs were used. The sample solution was added in the electrolyte media and the current was measured. The preparation and measurement of the training sets, test solutions and real samples, as well as the reference methods used, are detailed in the Supporting Information (Tables S1–4).

3. Results and discussion

3.1. Optimization of individual sensors

In conventional OECTs the voltage gradient between G and the channel controls the response. V_g regulates the migration of cations into and out of the channel, thus controlling its electronic electrical conductivity. For this reason, OECT sensing strategies are normally focused on the functionalization of the gate, in order create an analyte-dependent V_g. In these approaches, the sensitivity is directly linked to the transconductance, g_m:

$$g_m = \frac{\partial I_d}{\partial V_g}$$

Early attempts have shown that this strategy is not effective when using ISM. Due to their high impedance, electrodes coated with a polymeric membrane show a very large capacitance. This situation must be avoided, since it is well known that the capacitance of the gate negatively affects the OECT sensor performance [18]. Indeed, since V_g is the source of the controlled ion migration into the channel, any capacitive loss between the gate and the channel will result in a weaker gating effect. Ideally, most of the gate potential should drop in the proximity of the channel. A large gate capacitance will produce a significant drop of potential in the vicinity of the gate, resulting in a very weak driving force for the migration of ions. This issue has been recognized and address by depositing the ISM on top of the channel [30–32]. We have recently shown that a suitable combination of a thick PEDOT:PSS film in the channel and an adjusted membrane composition allows obtaining high sensitivities for the determination of ions such as K^+ [17]. Interestingly, we have also shown that maximum sensitivity is achieved for $V_g = 0$ V. Since the gate voltage measures the bias with respect to the S electrode, which is grounded, it means that minimal V_g are required. In other words, the polarization of the solution-membrane interface produced by the selective extraction of ions creates an electrical field that can modulate the channel conductivity. As a downside, these systems display a relatively high response time. Therefore, some initial work was focused on finding a balance between optimization of the sensitivity and minimization of the response time.

To test the effect of the concentration of the conducting polymer, different IS-OECTs for K^+ were built using channels made with PEDOT:PSS at 0.2, 0.4, 0.8 and 3.5 %. Calibration curves for K^+ (at $V_g = 0$ V) show that both, the sensitivity, and the response time sharply increase with the percentage of the conductive polymer (Fig. 3A–B). One of the main characteristics of OECTs is their volumetric capacitance, which means that their gating mechanism -controlled by the migration of cations-is heavily influenced by the thickness and density of the channel. Based on these results, a percentage of 0.4 % PEDOT:PSS was considered to provide good sensitivity (600 μA/decade) while offering also reasonable response time (Fig. 3B). For the rest of the experiments channels made with a 0.4 % PEDOT:PSS were used. A study of the thickness of the PEDOT:PSS film, transconductance and analytical performance are detailed in Supporting Information (Figs. S4 and S5).

Additional experiments were also performed to evaluate the effect of approaches to enhance the conductivity of the channel, such as the addition of DMSO. Treatments with DMSO have been shown to induce conformational changes in the polymer, leading to a significant increase in conductivity. This should lead to an improvement on the sensitivity. *Blom et al.* studied the effect of DMSO deposition on thick films of PEDOT:PSS [28]. For channels made with 0.4 % PEDOT:PSS we have found that the DMSO treatment does not show any significant improvement neither on the channel conductivity nor the sensitivity. Nevertheless, DMSO treatment has a positive effect on the stability of the sensor. In general, it is observed a reduction in the 1/f noise, with an enhance long-term baseline stability. For instance, for transistors made with 0.4 % PEDOT:PSS, a drift in the baseline of 0.032 mA/minute was originally observed. However, for the same type of transistor, the treatment with DMSO reduces the drift to 0.017 mA/minute (more details on this point calculation can be found in the SI, DMSO section). Also, a lower sensor to sensor variability is obtained and the response time was slightly improved.

3.2. Electrical characterization

K^+ sensors built using the DMSO treated channels were tested in a 0.1 M KCl solution. First, the current-voltage response of a bare channel and a membrane-coated channel were evaluated without using a gate. The addition of the membrane does not seem to produce a significant effect on the channel electrical characteristics. Both systems show a similar profile, with an ohmic behavior and fast response time (Fig. S6). Thereafter, the transconductance was evaluated using a Ag/AgCl gate, scanning V_g from −0.2 to 0.9 V ($V_d = -0.4$ V). The results (Fig. 4A–B) show that the bare channel shows a maximum transconductance ($g_{m\text{-}MAX}$) at approximately 0.3 V, which is consistent with previous reports [17]. For the IS-OECT, $g_{m\text{-}MAX}$ is found at values close to 0 V. The transconductance shows a bimodal behavior. It decreases in the range $0 < V_g < 0.6$ V, and then increases again. This pattern has been ascribed to the non-selective ion migration into the membrane at high V_g. Similar results have been obtained for sodium and ammonium cations.

Calibration curves were then performed at $V_g = 0$ V ($V_d = -0.4$ V). Fig. 5A shows a typical time trace upon additions of increasing concentration of potassium (similar results can be seen for other ions, see Fig. S7). As a preliminary assessment of the sensor-to-sensor variability, five different sensors were used. The slopes obtained for each sensor were very similar, with an average value of 605 μA/decade. However, the small differences in the channel initial resistance introduce variabilities in the initial current that increase the sensor-to-sensor

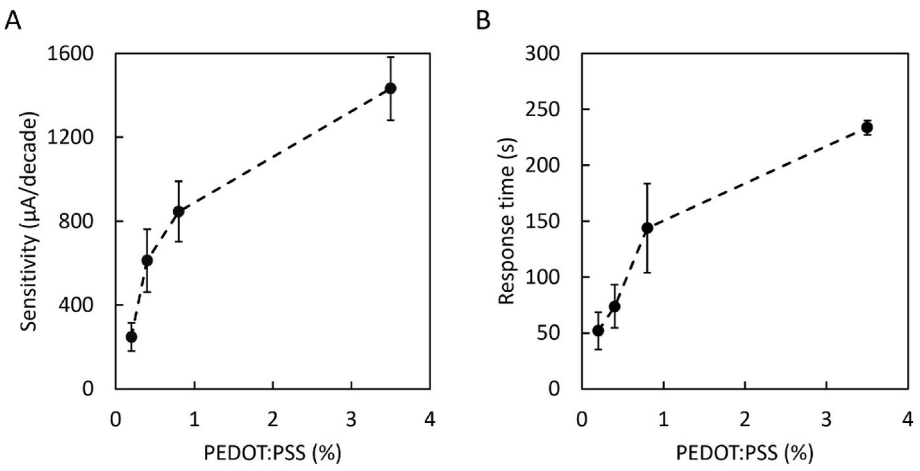

Fig. 3. (A) Influence of the PEDOT:PSS percentage on the sensitivity calculated between 10^{-4} – 10^{-1} M (the error bars correspond to standard deviation of six sensors). (B) Mean response time to obtain 95 % of total response between 10^{-4} – 10^{-1} M depending on PEDOT:PSS percentage (the error bars correspond to standard deviation of the different additions). The PEDOT:PSS percentages for both plots are: 0.2, 0.4, 0.8 and 3.5 %.

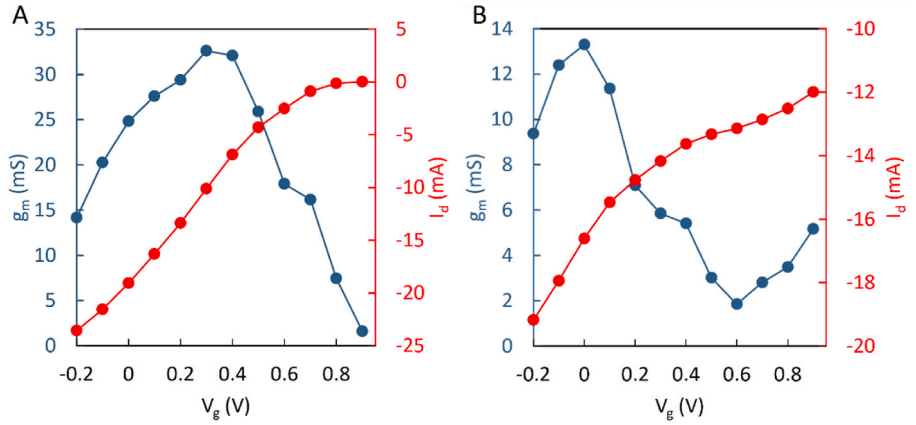

Fig. 4. (A) Transconductance (g_m) vs gate voltage (V_g) (blue) and drain current (I_d) vs gate voltage (V_g) (red) for a channel (drain voltage, V_d = −0.4 V). (B) Transconductance (g_m) vs gate voltage (V_g) (blue) drain current (I_d) vs gate voltage (V_g) (red) for a sensor (drain voltage, V_d = −0.4 V).

variability. To overcome this issue, instead of adjusting the voltage, the initial current I_d was adjusted. The current was set at the same value for all sensors (by slightly adjusting V_d) to an initial I_d = 15 mA. The resulting calibration plots are shown in Fig. 5B, which displays a significant reduction of the variability of the calibration plots when using different sensors. With this approach, an average sensitivity of 745 µA/decade, with a sensor-to-sensor variability for a given signal in the order of 8 % is obtained.

To reduce the instrumental complexity of the system, the elimination of the gate power supply was also explored (Fig. 5C). Indeed, with a $V_{g\text{-}MAX}$ close to 0 V, the optimum gate potential is very close to ground. Thus, since the source electrode is also grounded, the gate electrode was connected to the source. This leads to a more compact system where only one power supply is needed [17,33,34] The results of this change show that eliminating the gate power supply only produces a constant offset of the results but has a small effect on the analytical performance. In fact, using only one power supply slightly reduces the baseline noise level, probably due to eliminations of ground loops. This approach yielded similar results for the different ions tested. The results of the optimization of the analytical performance for each individual sensor with a grounded gate electrode are shown in Fig. 5D. The results of the optimization of the analytical performance for each individual sensor with a grounded gate electrode are shown in Fig. 5D. The comparison between the analytical performance of the IS-OECTs and the conventional ISEs is detailed in Table S5. In terms of the linear range and the limits of detection, our work is comparable with previous reports in OECT and ISE. Regarding sensitivity, a substantial improvement is observed except in the case of the system made by Clua *et al.* [17].

Seven consecutive calibrations were performed using the same sensor. The sensor showed good repeatability in the order of 4 % of error in terms of sensitivity. Higher variability was found at higher concentrations (Figs. S7A–C, Table 1). Thereafter, calibrations were performed using 5 different sensors (Figs. S8A–C). Table 1 shows the results of the intermediate precision of system. A very good intermediate precision of the analytical performance in the order of 5 % of error in terms of sensitivity between five different sensors was observed.

Response time was evaluated at 95 % of maximum response. As it is common in this type of systems, the response time increases as concentration decreases (Fig. S9). In general, response times in the 35–75 s range are observed. For ammonium, for example, a response time of 97 s is obtained for a 10^{-5} M addition. This can be considered an upper limit of the response time.

Selectivity was assessed by evaluating the response to the primary ion in the presence of typical interfering cations (K^+, Na^+, NH_4^+ and Ca^{2+}). For a solution with the ions present at 0.1 M concentration, the response was evaluated at different V_g. The main objective of this experiments is to evaluate what is the total effect produced in the response (I_d) when the interfering ion is added. While this is not a rigorous

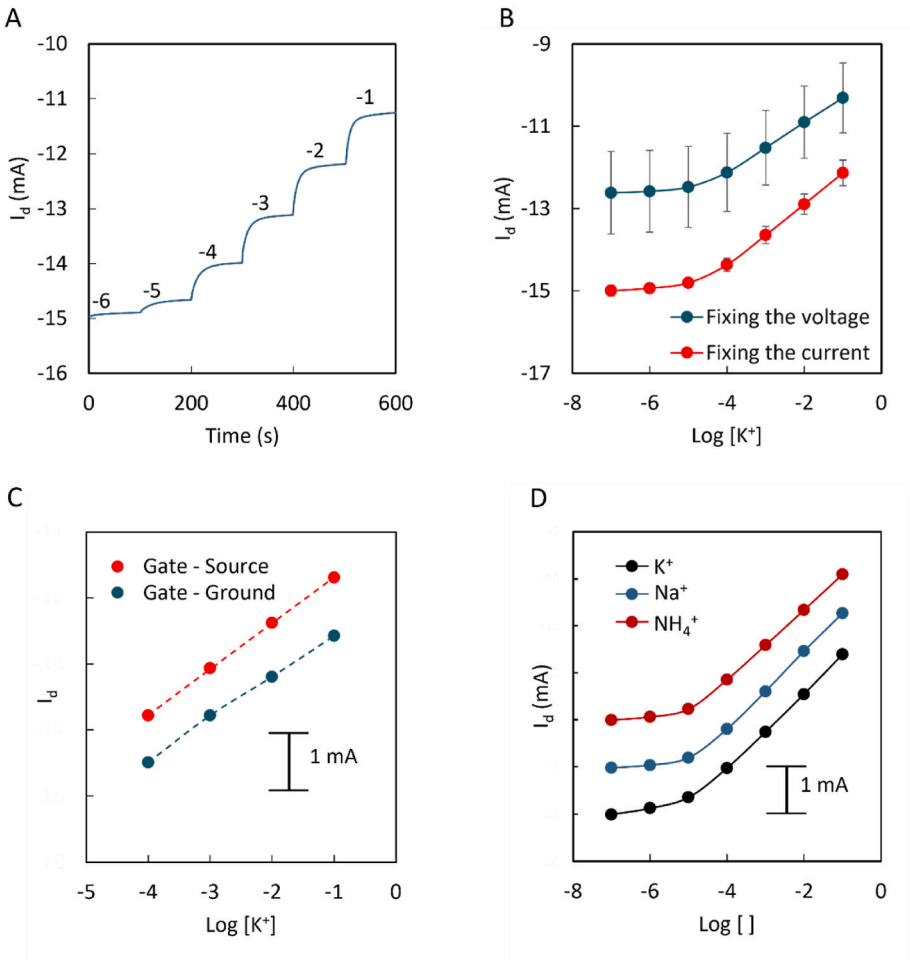

Fig. 5. (A) Typical time trace drain current (I_d) vs time in the different additions at voltage drain (V_d) = −0.4 V and voltage gate (V_g) = 0 V for K^+. (B) Calibration curves by applying voltage drain (V_d) = −0.4 V and voltage gate (V_g) = 0 V (blue) and by fixing the initial current in −15 mA (red) (error bars correspond to the standard deviation between five sensors). (C) Potassium calibration curves: gate connected to the source (red), gate connected to the ground (blue). (D) Calibration curves for each analyte.

Table 1
Repeatability and intermediate precision in terms of sensitivity for each IS-OECT. For potassium and sodium sensors the sensitivity value is calculated from 10^{-4} to 10^{-1} and for ammonium sensors from 10^{-5} to 10^{-1}.

	Repeatability (μA/dec)	Intermediate precision (μA/dec)
K^+ OECT	857.65 ± 27.96	807.34 ± 34.45
Na^+ OECT	896.22 ± 51.08	811.39 ± 47.87
NH_4^+ OECT	778.75 ± 27.96	833.29 ± 33.11

approach, it provides a good approximation. The results -measured as the subtraction of the final value of I_d at the end of the calibration (I_f) from the initial value of the current prior to performing the calibration (I_0)- (Fig. 6A–C) show that all ions have a maximum response at $V_g = 0$ V. This can be explained since there is a spontaneous extraction of ions driven by thermodynamic factors (ion-ionophore equilibrium constant). For higher voltages (V_g = 0.7 V), the incorporation of ions into the membrane are controlled by the hydration energies (lipophilicity) of the cation. Also, they show that the only significant interference effect is observed between K^+ and NH_4^+. This is a typical interference commonly observed in ISEs, which stems from the similarity in the charge-size ratio of these two ions. Unfortunately, models used for calculating selectivity coefficients in ISEs cannot be applied in these conditions. The qualitative assessment of selectivity performed here compares the variation in I_d produced by the addition of the ions at different V_g values. Interestingly, these results show that at low V_g the molecular recognition of the ISM controls the response, with a highest selectivity obtained for $V_g = 0$ V.

The ability to provide precise and reliable results is a key point in this work. For this, two levels of concentrations were studied: low level ($5{\cdot}10^{-4}$ M) and medium-high level ($1{\cdot}10^{-2}$ M). For each concentration, 5 sensors were prepared for each analyte and were measured under conditions of maximum variability (intermediate precision with different days, sensors, and instruments). Likewise, the variability associated with the repeatability of each sensor was studied. To do this test, first a calibration was carried out to know the current value for each concentration setting the baseline at −15 mA. The sensor was then rinsed, the selected initial current value was set and an addition of a solution of the desired concentration was performed. This process was repeated different times. The precision of the sensors was evaluated at 95 % of the final response. Table 2 and Fig. S6 show the percentage of precision error (in terms of concentration) associated with low and high concentrations. Table 2 show the precision studies for two additions and Table S6 for three additions.

To evaluate the sensor response over a number of days, 4 different sensors for each analyte were calibrated on different days. The calibration was always preceded by a conditioning (1 h in 0.1 M XCl, X being the analyte of interest). These results are seen in Figs. S10A–C. It was concluded that the sensors maintain their analytical performance for at least 20 days.

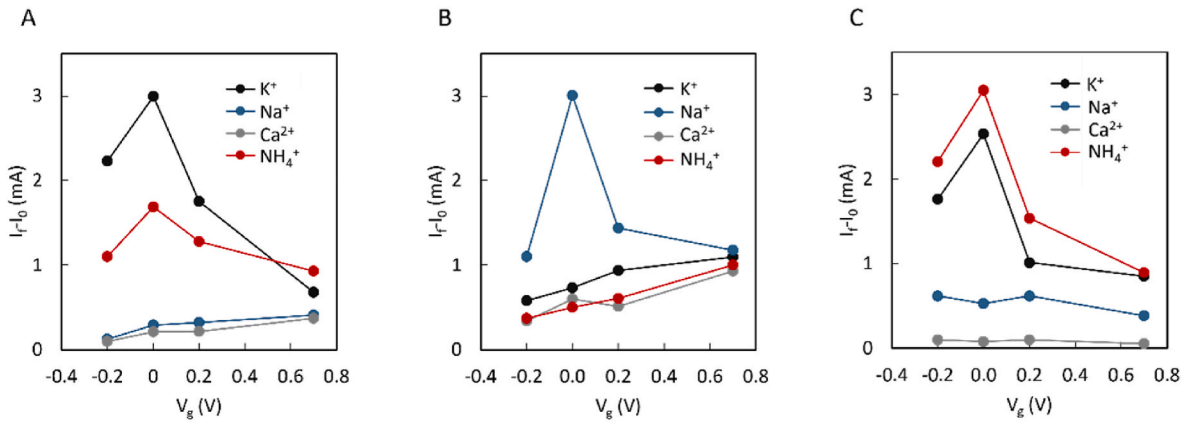

Fig. 6. Selectivity studies: total response I_f-I_0 for the evaluation of interfering effect in the IS-OECT as a function of voltage gate (V_g) (voltage drain, $V_d = -0.4$) (A) In a potassium OECT. (B) In a sodium OECT. (C) In an ammonium OECT.

Table 2
Precision studies of two additions between the same sensor and between sensors in low and high level of concentration with 5 sensors, 5 days and 3 instruments.

	Low concentration level ($5{\cdot}10^{-4}$ M)		High concentration level ($1{\cdot}10^{-2}$ M)	
	Intermediate precision	Repeatability	Intermediate precision	Repeatability
K^+ OECT	11.41 %	6.35 %	11.37 %	6.30 %
Na^+ OECT	10.02 %	3.11 %	11.97 %	6.34 %
NH_4^+ OECT	14.55 %	3.83 %	11.98 %	8.49 %

3.3. The OECT array

The functionalization of the channel -instead of the gate-provides a multiplex advantage, since several channels can be simultaneously used in the same solution using the same gate. To prove this point, 3 channels -each with a different ISM-were used, and a Ag/AgCl gate was connected to the source of each sensor, as shown in Fig. 2B. Multivariate calibration can help to overcome problems of selectivity of each individual sensor (Figs. S11A–C).

3.4. Construction and validation of the PLS model

PLS was used to correlate the concentration of ammonium, potassium, and sodium in the different samples (expressed as logarithm of concentration) with the three recorded I_d values. A PLS model was constructed for each one of the three target analytes using the 33 samples of the training set. The goodness of fit between the data and the calibration model is measured by Root Mean Square Error of Calibration (RMSEC). Two factors explained 96.87 %, 97.25 % and 95.28 % of the original information in ammonium, potassium and sodium respectively, with a root mean square error of cross validation (RMSECV) of 0.1242, 0.1314, 0.1329. RMSECV is expressed in logarithmic concentration units, representing the average errors in quantifying the target analytes using the derived models. Although RMSECV, which corresponds to the internal validation since this technique uses for validation the same samples that have been used in the construction of the model, has limitations due to the estimation of the error in the same magnitude at low and high concentrations, it is widely used as a figure of merit in model comparison [35].

For the external validation, the whole set of samples were divided into a training set (60 % of the samples, 33 samples) and a test set (40 % of the samples, 22 samples). These samples were selected ensuring that all the concentrations levels were present in the training and set samples. The goodness of prediction is calculated using the root mean square error of prediction (RMSEP) of the test set and shows the ability of the model for the prediction of new samples that have not been used during the construction of the multivariate model. Table 3 shows the figures of merit of the optimum multivariate models.

For the comparison with reference methods, 15 real samples were measured with the OECTs array and with two reference techniques: Fluorescence for ammonium and AES for potassium and sodium.

3.5. Validation from reference techniques

To compare the results obtained with each PLS model using the OECTs and the reference method used for the analysis of each one of the target analytes, we used a linear approach with the joint confidence interval for the intercept and the slope [36]. The theoretical regression line obtained with the analysis of the saliva samples using the reference method and the PLS model for a specific ion should have intercept = 0 and slope = 1 if the predictions of the two methods (reference method and PLS model) were identical. Therefore, if the two sets of predictions provide comparable results, the joint confidence interval of the intercept and the slope of the regression line between the two methods has to include the theoretical point (0, 1) for a α significance level. Fig. 7A–F shows the three regression lines between the reference methods and the PLS models using the OECTs, and the resulting joint confidence intervals for the intercept and the slope, showing that there is no statistically significant difference between the different sets of predictions at a significance level α = 5 %

4. Conclusions

A novel array consisting of three single OECTs connected to a single gate was prepared and characterized. This allows the instrumental equipment to be reduced. Regarding the measurement of the sample,

Table 3
Figures of merit of multivariate model.

Analyte	RMSEC	RMSECV	R^2 (Cal, CV)	RMSEP	Prediction Bias	R^2 (Pred)
NH_4^+	0.11694	0.12418	0.969, 0.965	0.13088	0.01346	0.968
K^+	0.11813	0.13136	0.973, 0.966	0.13564	−0.034743	0.967
Na^+	0.11909	0.13286	0.953, 0.941	0.11985	−0.028093	0.953

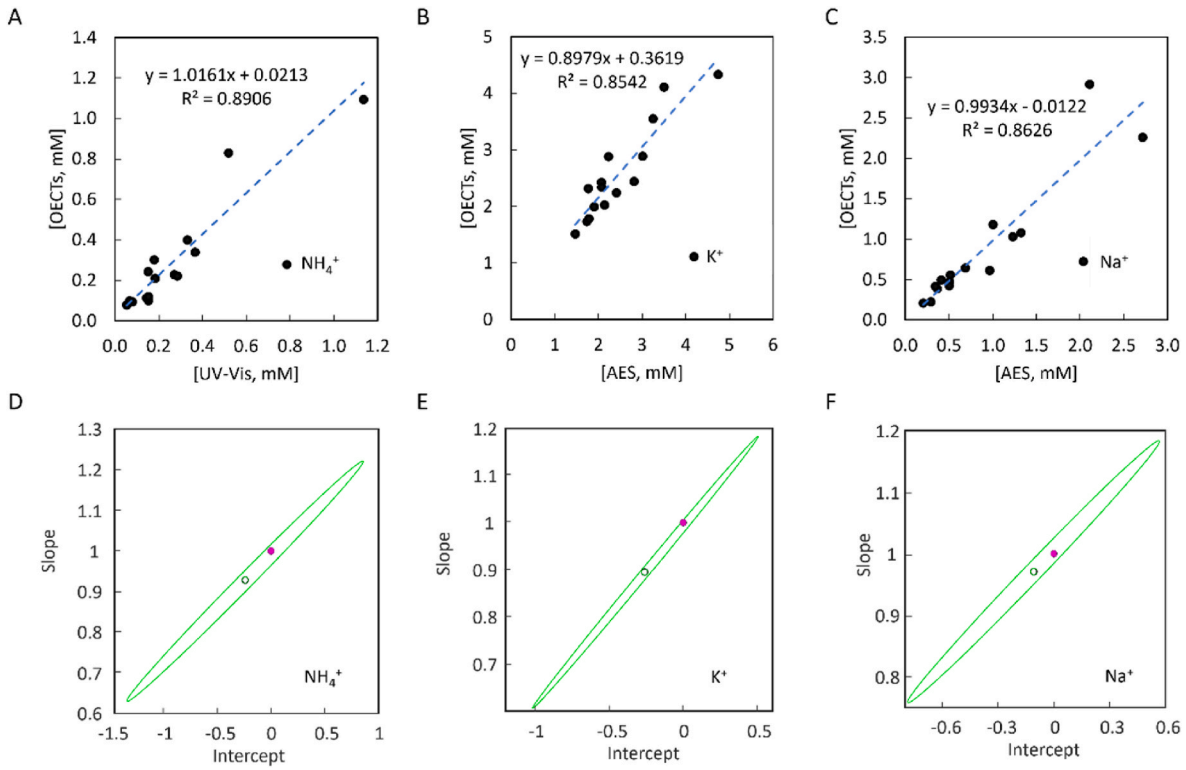

Fig. 7. Regression line between the reference results and multivariate model results for OECTs. (A) Ammonium. (B) Potassium. (C) Sodium. Joint confidence intervals for the intercept and the slope. (D) Ammonium. (E) Potassium. (F) Sodium.

this design allows the sample to be measured instantly. The sensors offer high precision in the maximum conditions of variability, being suitable for ion analysis. Furthermore, due to the use of low-cost substrates such as paper, it presents significant advantage compared to other instrumental devices for similar analyzes such as fluorescence and AES.

Finally, the use of multivariate models has been crucial to properly extract the information of each OECT, predict and quantify selectively the concentrations of each biomarker. The results obtained by the OECTs have been compared with those obtained by the reference methods. A high accuracy of the sensors has been demonstrated for the three analytes. It could be expected that through the addition of one blank sensor with an ionophore-free membrane in the sensor array, the noise will be reduced, and the precision and the robustness of the method will improve.

CRediT authorship contribution statement

Ariadna Dasca: Writing – original draft, Investigation. **Pascal Blondeau:** Writing – review & editing, Supervision, Investigation. **Jordi Riu:** Writing – review & editing, Supervision, Investigation. **Francisco J. Andrade:** Writing – review & editing, Supervision, Funding acquisition, Conceptualization.

Declaration of competing interest

The authors declare that they have no known competing financial interests or personal relationships that could have appeared to influence the work reported in this paper.

Data availability

Data will be made available on request.

Acknowledgments

The authors acknowledge the financial support from the Spanish Ministry of Science, Innovation and Universities (MICIU), the State Research Agency (AEI) and the European Regional Development Fund (ERDF), EU: PID2022-136649OB-I00, PID2019-106862RB-I00/AEI/10.13039/501100011033, PDC2021-120921-I00. Chemometrics and Sensorics for Analytical Solutions (CHEMOSENS, ref.2021 SGR 00705, Departament de Recerca i Universitats, Generalitat de Catalunya). Ariadna Dasca Beneito would like to thank the Universitat Rovira i Virgili, for the financial support through the scholarship 2021PMF-PIPF-21, Martí i Franquès program.

Appendix A. Supplementary data

Supplementary data to this article can be found online at https://doi.org/10.1016/j.talanta.2024.126957.

References

[1] S.K. Vashist, P.B. Luppa, L.Y. Yeo, A. Ozcan, J.H.T. Luong, Emerging technologies for next-generation point-of-care testing, Trends Biotechnol. 33 (2015) 692–705, https://doi.org/10.1016/j.tibtech.2015.09.001.

[2] P. Sengupta, K. Khanra, A.R. Chowdhury, P. Datta, Lab-on-a-chip Sensing Devices for Biomedical Applications, Elsevier Ltd, 2019, https://doi.org/10.1016/B978-0-08-102420-1.00004-2.

[3] J.R. Huizenga, C.H. Gips, Determination of ammonia in saliva using indophenol, an ammonium electrode and an enzymatic method: a comparative investigation, Clin. Chem. Lab. Med. 20 (1982) 571–574, https://doi.org/10.1515/cclm.1982.20.8.571.

[4] A. Corba, A.F. Sierra, P. Blondeau, B. Giussani, J. Riu, P. Ballester, F.J. Andrade, Potentiometric detection of creatinine in the presence of nicotine: molecular recognition, sensing and quantification through multivariate regression, Talanta 246 (2022) 123473, https://doi.org/10.1016/j.talanta.2022.123473.

[5] M. Gutiérrez, S. Alegret, M. del Valle, Bioelectronic tongue for the simultaneous determination of urea, creatinine and alkaline ions in clinical samples, Biosens. Bioelectron. 23 (2008) 795–802, https://doi.org/10.1016/j.bios.2007.08.019.

[6] P. Pirovano, M. Dorrian, A. Shinde, A. Donohoe, A.J. Brady, N.M. Moyna, G. Wallace, D. Diamond, M. McCaul, A wearable sensor for the detection of sodium

and potassium in human sweat during exercise, Talanta 219 (2020) 121145, https://doi.org/10.1016/j.talanta.2020.121145.
[7] J. Kim, A.S. Campbell, B.E.F. de Ávila, J. Wang, Wearable biosensors for healthcare monitoring, Nat. Biotechnol. 37 (2019) 389–406, https://doi.org/10.1038/s41587-019-0045-y.
[8] H. Derakhshandeh, S.S. Kashaf, F. Aghabaglou, I.O. Ghanavati, A. Tamayol, Smart bandages: the future of wound care, Trends Biotechnol. 36 (2018) 1259–1274, https://doi.org/10.1016/j.tibtech.2018.07.007.
[9] W. Gao, S. Emaminejad, H.Y.Y. Nyein, S. Challa, K. Chen, A. Peck, H.M. Fahad, H. Ota, H. Shiraki, D. Kiriya, D.H. Lien, G.A. Brooks, R.W. Davis, A. Javey, Fully integrated wearable sensor arrays for multiplexed in situ perspiration analysis, Nature 529 (2016) 509–514, https://doi.org/10.1038/nature16521.
[10] L.L. Wang, W.B.B. Ng, J.A. Jackman, N.J. Cho, Graphene-functionalized natural microcapsules: modular building blocks for ultrahigh sensitivity bioelectronic platforms, Adv. Funct. Mater. 26 (2016) 2097–2103, https://doi.org/10.1002/adfm.201504940.
[11] Y. Wang, H. Haick, S. Guo, C. Wang, S. Lee, T. Yokota, T. Someya, Skin bioelectronics towards long-term, continuous health monitoring, Chem. Soc. Rev. (2022) 3759–3793, https://doi.org/10.1039/d2cs00207h.
[12] J. Rivnay, S. Inal, A. Salleo, R.M. Owens, M. Berggren, G.G. Malliaras, Organic electrochemical transistors, Nat. Rev. Mater. 3 (2018) 17086, https://doi.org/10.1038/natrevmats.2017.86.
[13] B.D. Paulsen, K. Tybrandt, E. Stavrinidou, J. Rivnay, Organic mixed ionic–electronic conductors, Nat. Mater. 19 (2020) 13–26, https://doi.org/10.1038/s41563-019-0435-z.
[14] D.A. Bernards, G.G. Malliaras, Steady-state and transient behavior of organic electrochemical transistors, Adv. Funct. Mater. 17 (2007) 3538–3544, https://doi.org/10.1002/adfm.200601239.
[15] E. MacChia, R.A. Picca, K. Manoli, C. Di Franco, D. Blasi, L. Sarcina, N. Ditaranto, N. Cioffi, R. Österbacka, G. Scamarcio, F. Torricelli, L. Torsi, About the amplification factors in organic bioelectronic sensors, Mater. Horiz. 7 (2020) 999–1013, https://doi.org/10.1039/c9mh01544b.
[16] A. Ait Yazza, P. Blondeau, F.J. Andrade, Simple approach for building high transconductance paper-based organic electrochemical transistor (OECT) for chemical sensing, ACS Appl. Electron. Mater. 3 (2021) 1886–1895, https://doi.org/10.1021/acsaelm.1c00116.
[17] M. Clua Estivill, A. Ait Yazza, P. Blondeau, F.J. Andrade, Ion-selective organic electrochemical transistors for the determination of potassium in clinical samples, Sensor. Actuator. B Chem. 401 (2024) 135027, https://doi.org/10.1016/j.snb.2023.135027.
[18] Z. Mousavi, A. Ekholm, J. Bobacka, A. Ivaska, Ion-selective organic electrochemical junction transistors based on poly(3,4-ethylenedioxythiophene) doped with poly (styrene sulfonate), Electroanalysis 21 (2009) 472–479, https://doi.org/10.1002/elan.200804427.
[19] M. Sessolo, J. Rivnay, E. Bandiello, G.G. Malliaras, H.J. Bolink, Ion-selective organic electrochemical transistors, Adv. Mater. 26 (2014) 4803–4807, https://doi.org/10.1002/adma.201400731.
[20] S.I. Khamees, Evaluation of inorganic ions and enzymes levels in saliva of patients with chronic periodontitis and healthy subjects, J. Bagh. Coll. Dent. 24 (2012) 93–97.
[21] C. Seethalakshmi, D. Koteeswaran, V. Chiranjeevi, Correlation of serum and salivary biochemical parameters in end stage renal disease patients undergoing hemodialysis in pre and post-dialysis state, J. Clin. Diagn. Res. 8 (2014) CC12–CC14, https://doi.org/10.7860/JCDR/2014/10404.5306.
[22] A.C. Gonçalves, F.A.L. Marson, R.M.H. Mendonça, C.S. Bertuzzo, I.A. Paschoal, J. D. Ribeiro, A.F. Ribeiro, C.E. Levy, Chloride and sodium ion concentrations in saliva and sweat as a method to diagnose cystic fibrosis, J. Pediatr. 95 (2019) 443–450, https://doi.org/10.1016/j.jped.2018.04.005.
[23] C. Labat, S. Thul, J. Pirault, M. Temmar, S.N. Thornton, A. Benetos, M. Bäck, Differential associations for salivary sodium, potassium, calcium, and phosphate levels with carotid intima media thickness, heart rate, and arterial stiffness, Dis. Markers 2018 (2018), https://doi.org/10.1155/2018/3152146.
[24] F.M. Schmidt, O. Vaittinen, M. Metsälä, M. Lehto, C. Forsblom, P.H. Groop, L. Halonen, Ammonia in breath and emitted from skin, J. Breath Res. 7 (2013) 017109, https://doi.org/10.1088/1752-7155/7/1/017109.
[25] G. Bilancio, P. Cavallo, C. Lombardi, E. Guarino, V. Cozza, F. Giordano, G. Palladino, M. Cirillo, Saliva for assessing creatinine, uric acid, and potassium in nephropathic patients, BMC Nephrol. 20 (2019) 1–9, https://doi.org/10.1186/s12882-019-1437-4.
[26] M. Wesoły, X. Cetó, M. delValle, P. Ciosek, W. Wróblewski, Quantitative analysis of active pharmaceutical ingredients (APIs) using a potentiometric electronic tongue in a SIA flow system, Electroanalysis 28 (2016) 626–632, https://doi.org/10.1002/elan.201500407.
[27] A. Haleem, M. Javaid, R.P. Singh, R. Suman, Telemedicine for healthcare: capabilities, features, barriers, and applications, Sens. Int. 2 (2021) 100117, https://doi.org/10.1016/j.sintl.2021.100117.
[28] L.V. Lingstedt, M. Ghittorelli, H. Lu, D.A. Koutsouras, T. Marszalek, F. Torricelli, N. I. Crăciun, P. Gkoupidenis, P.W.M. Blom, Effect of DMSO solvent treatments on the performance of PEDOT:PSS based organic electrochemical transistors, Adv. Electron. Mater. 5 (2019) 1–8, https://doi.org/10.1002/aelm.201800804.
[29] F. Torricelli, D.Z. Adrahtas, Z. Bao, M. Berggren, F. Biscarini, A. Bonfiglio, C. A. Bortolotti, C.D. Frisbie, E. Macchia, G.G. Malliaras, I. McCulloch, M. Moser, T. Q. Nguyen, R.M. Owens, A. Salleo, A. Spanu, L. Torsi, Electrolyte-gated transistors for enhanced performance bioelectronics, Nat. Rev. Methods Primers 1 (2021) 1–54, https://doi.org/10.1038/s43586-021-00065-8.
[30] N. Coppedè, M. Giannetto, M. Villani, V. Lucchini, E. Battista, M. Careri, A. Zappettini, Ion selective textile organic electrochemical transistor for wearable sweat monitoring, Org. Electron. 78 (2020) 105579, https://doi.org/10.1016/j.orgel.2019.105579.
[31] P. Romele, P. Gkoupidenis, D.A. Koutsouras, K. Lieberth, Z.M. Kovács-Vajna, P.W. M. Blom, F. Torricelli, Multiscale real time and high sensitivity ion detection with complementary organic electrochemical transistors amplifier, Nat. Commun. 11 (2020) 1–11, https://doi.org/10.1038/s41467-020-17547-0.
[32] S. Wustoni, C. Combe, D. Ohayon, M.H. Akhtar, I. McCulloch, S. Inal, Membrane-free detection of metal cations with an organic electrochemical transistor, Adv. Funct. Mater. 29 (2019) 1–10, https://doi.org/10.1002/adfm.201904403.
[33] X. Ji, X. Lin, J. Rivnay, Organic electrochemical transistors as on-site signal amplifiers for electrochemical aptamer-based sensing, Nat. Commun. 14 (2023) 1665, https://doi.org/10.1038/s41467-023-37402-2.
[34] S. Han, S. Yamamoto, A.G. Polyravas, G.G. Malliaras, Microfabricated ion-selective transistors with fast and super-nernstian response, Adv. Mater. 32 (2020) 1–8, https://doi.org/10.1002/adma.202004790.
[35] H. Parastar, D. Kirsanov, Analytical figures of merit for multisensor arrays, ACS Sens. 5 (2020) 580–587, https://doi.org/10.1021/acssensors.9b02531.
[36] J. Riu, F.X. Rius, Assessing the accuracy of analytical methods using linear regression with errors in both axes, Anal. Chem. 68 (1996) 1851–1857, https://doi.org/10.1021/ac951217s.